The Meteoritical Society

Meteoritics & Planetary Science 50, Nr 4, 632–648 (2015)
doi: 10.1111/maps.12363

Geochemical diversity of shergottite basalts: Mixing and fractionation, and their relation to Mars surface basalts

Allan H. TREIMAN[1*] and Justin FILIBERTO[2]

[1]Lunar and Planetary Institute, 3600 Bay Area Boulevard, Houston, Texas 77058, USA
[2]Department of Geology, Southern Illinois University, Carbondale, Illinois 62901, USA
[*]Corresponding author. E-mail: treiman@lpi.usra.edu

(Received 16 March 2014; revision accepted 09 July 2014)

Abstract–The chemical compositions of shergottite meteorites, basaltic rocks from Mars, provide a broad view of the origins and differentiation of these Martian magmas. The shergottite basalts are subdivided based on their Al contents: high-Al basalts (Al > 5% wt) are distinct from low-Al basalts and olivine-phyric basalts (both with Al < 4.5% wt). Abundance ratios of highly incompatible elements (e.g., Th, La) are comparable in all the shergottites. Abundances of less incompatible elements (e.g., Ti, Lu, Hf) in olivine-phyric and low-Al basalts correlate well with each other, but the element abundance ratios are not constant; this suggests mixing between components, both depleted and enriched. High-Al shergottites deviate from these trends consistent with silicate mineral fractionation. The "depleted" component is similar to the Yamato-980459 magma; approximately, 67% crystal fractionation of this magma would yield a melt with trace element abundances like QUE 94201. The "enriched" component is like the parent magma for NWA 1068; approximately, 30% crystal fractionation from it would yield a melt with trace element abundances like the Los Angeles shergottite. This component mixing is consistent with radiogenic isotope and oxygen fugacity data. These mixing relations are consistent with the compositions of many of the Gusev crater basalts analyzed on Mars by the Spirit rover (although with only a few elements to compare). Other Mars basalts fall off the mixing relations (e.g., Wishstone at Gusev, Gale crater rocks). Their compositions imply that basalt source areas in Mars include significant complexities that are not present in the source areas for the shergottite basalts.

INTRODUCTION

Our understanding of Martian magmas and geochemistry began with multielement analyses of lunar samples (e.g., Wänke et al. 1972, 1973) and then of the "SNC" meteorites (e.g., Burghele et al. 1983; Dreibus and Wänke 1985; Wänke and Dreibus 1988), from recognition that they were samples of Mars (Bogard and Johnson 1983; see Treiman et al. 2000). Regularities observed in element abundances ratios were used to tease apart several effects on the compositions of basalts and their source mantles: igneous silicate fractionations; depletions of siderophile elements, which were ascribed to core formation; and depletions of cosmochemically volatile elements, which were ascribed to processes during planetary accretion. This work was pioneered by the Mainz group under Dr. H. Wänke (e.g., Wänke 1981). Dr. Michael Drake and his group at The University of Arizona also investigated chemical regularities in planetary basalts especially as they pertained to siderophile elements and the compositions of planetary cores (e.g., Jones 1984; Treiman et al. 1986, 1987; Jones and Drake 1993; Righter and Drake 1997; Drake 2000; Drake and Righter 2002), and performed laboratory experiments to constrain the conditions of core formation behind the observed element patterns (e.g., Newsom and Drake 1982; Hillgren et al. 1996; Righter and Drake 2003).

These works on multielement chemistry of the Martian meteorites focused mostly on whole-planet

properties, i.e., depletion in volatile elements dating from accretion, and depletion in siderophile elements dating from core formation. Silicate fractionations were viewed essentially as confounding effects—to be "seen through" wherever possible. Thus, Treiman et al. (1986) and Treiman (2003) divided the igneous incompatible elements into two groups depending on their incompatibility, and examined depletions in volatile and siderophile elements within each group. Comparing elements between the groups yielded poor correlations, and thus poor constraints on depletion factors for volatile and siderophile elements. This separation according to igneous incompatibility is more pronounced in Earth basalts, e.g., in MORBs, which derive from strongly depleted sources. Thus, for instance, the mantle abundance of the moderately siderophile element Mo can be estimated from the Mo/Nd ratio because it is fairly constant among primitive Earth basalts (Newsom and Palme 1984); other similar ratios are not constant, e.g., Mo/U because of differences in igneous incompatibility.

Early studies of Martian basalt geochemistry considered all known meteorite types (shergottites, nakhlites, and Chassigny) without strong distinctions among them, and between which meteorites represented magma compositions and which were cumulate rocks (Treiman et al. 1986, 1987; Dreibus and Wänke 1987, 1990; Wänke and Dreibus 1988). Few Martian meteorites were known in those years, but many more are known now, which allows (and demands) some specificity. Treiman (2003) restricted his geochemical study to the shergottites, including the cumulate lherzolites, but leaving out other cumulate lithologies (nakhlites, Chassigny, and ALH84001). In the previous year, olivine-phyric shergottites had been recognized as a separate group (Goodrich 2002); they are now the most common type of shergottite. Several of the olivine-phyric shergottites have been shown to represent magma compositions or nearly so (Y-980459, NWA 5789, NWA 6234, LAR 06319: Musselwhite et al. 2006; Peslier et al. 2010; Filiberto and Dasgupta 2011; Filiberto et al. 2012; Gross et al. 2013), and the others are either uncertain or inferred to contain some excess olivine relative to a melt composition, either as cognate cumulate grains or as xenocrysts (see Filiberto et al. 2010a). The newly recognized Martian meteorite NWA 7034 (and its pairs) is a polymict basaltic breccia, and has expanded the known range of Martian lithologies (Agee et al. 2013).

As in Treiman (2003), this study is restricted to the shergottites alone—those with compositions that represent magmas, or nearly so. We include all olivine-phyric shergottites, recognizing that several of them may contain some excess olivine; because we emphasize elements that are incompatible in olivine, the effects of excess olivine will be limited. The lherzolitic shergottites are cumulate rocks as is ALH 84001; both are excluded. The nakhlites and chassignites are also cumulate rocks (rich in augite and olivine, respectively), and are excluded. These groups may be closely related (McCubbin et al. 2013), but are distinct from the shergottites in their trace element signatures and radiogenic isotope characteristics (Borg et al. 2003). And, of course, NWA 7034 and its pairs are excluded because they are a polymict breccia (Agee et al. 2013). The shergottites are not the only analyzed Martian basalts—several have been analyzed on Mars for major and minor elements by instruments on rover missions: Mars Pathfinder, Opportunity, Spirit, and Curiosity. We will return to these Martian in situ analyses later.

Implicit in these earlier treatments of igneous incompatible elements was that their abundances (after planetary accretion and core formation) had been modified only by simple silicate igneous fractionations. To understand abundances of a target element (volatile or siderophile), one had only to find a reference element (refractory and lithophile) of the same incompatibility with respect to simple processes like partial melting of lherzolitic mantle or crystallization of olivine and pyroxenes.

This view, that diversity in the shergottites was caused only by simple igneous fractionation (e.g., Greenough and Ya'akoby 2013), is not consistent with extensive evidence for mixing of sources. The radiogenic isotope geochemistry of the shergottites ($^{147}Sm/^{144}Nd$, $^{87}Rb/^{86}Sr$, $^{176}Lu/^{177}Hf$; U-Th-Pb) is consistent with mixing of two source reservoirs—one depleted in igneous incompatible elements, and one enriched in them, with different isotopic characteristics and chemical characteristics like oxidation state (e.g., Shih et al. 1982; Jones 1989; Borg et al. 2003; Herd 2003; Foley et al. 2005; Blinova and Herd 2009). These two reservoirs must have been established early in Mars' history (e.g., Borg and Draper 2003; Borg et al. 2003; Foley et al. 2005; Debaille et al. 2008), possibly by planet-scale differentiation of a magma ocean, i.e., as cumulates and late-stage differentiate (like lunar KREEP). This two-component mixing was also apparent in the overall depletions in incompatible elements (by the abundance ratio La/Yb) and in the source magmas' oxygen fugacities (Herd et al. 2002; Herd 2003). Additional data, and analyses of newer Martian meteorites, have served to confirm the concept of two-component mixing (e.g., Bridges and Warren 2006; Borg et al. 2012; Shearer et al. 2013).

Here, we investigate how much of this mixing model of shergottite petrogenesis can be applied to

their bulk chemical compositions. The mixing relations have been shown consistent with at least one bulk geochemical parameter, La/Lu (Herd 2003), and our goal here was to investigate whether that simple mixing model can also explain abundances and abundance ratios of a broad range of elements. We focus on incompatible trace elements, but draw significant inferences from the major element Al and the compatible trace element Ni to explore the genetic relationships between olivine-phyric and basaltic shergottites. As a byproduct of this study, we suggest a subclassification of the shergottite meteorite basalts.

DATA SOURCES

This work relies on published chemical analyses of shergottite meteorites, both as compiled and in the original literature. Our recompilation of this data is given as Table S1, enlarged from that of Filiberto et al. (2012). In a few cases, we have calculated abundances of phosphorus (which is not commonly analyzed) from modal abundances of phosphate minerals (apatite and merrillite). For the Los Angeles meteorite, we have used data from the analyses of both Rubin et al. (2000) and Jambon et al. (2002), which are significantly different; e.g., the former shows 570 ppb Th, and the latter averages 810 ppb Th. We use the Jambon et al. (2002) analyses for all graphs except those involving phosphorus, for which no data were presented. In those cases only, we use the average of the two Rubin et al. (2000) analyses.

The quality of data in this compilation is variable, as can be seen by examining multiple published analyses of a single meteorite (e.g., EETA79001: Meyer 2012), and by comparison of independent analyses of supposedly paired meteorites (e.g., Irving et al. 2011; Filiberto et al. 2012). Treiman (2003) showed how this variability affects element correlations, even for elements that nominally should be sited in the same mineral (e.g., Th and La in phosphates). Variability can be even more striking when comparing elements that are sited in different solid phases, for instance Hf and Th; the former would concentrate in zircon or baddeleyite, and the latter in apatite or merrillite. Abundances of nickel are similarly problematic in the olivine-phyric basalts. In them, Ni is concentrated in the larger magnesian olivine grains, which are uncommon enough that an aliquot for analysis could reasonably contain more or less than the rock's overall average. The analyses used here (Table S1) are a compilation and average, and so avoid individual aberrant values.

RESULTS

Shergottite Classification

Before diving into the details of incompatible element geochemistry, we note an important distinction among shergottites that comes from consideration of their abundances of incompatible elements. For many shergottites, Al behaved as an incompatible element through most of their fractionation histories. Many shergottites have low Al abundances, and thus attained saturation with plagioclase only late in their fractionation (e.g., NWA 5789; Shergotty), and a few shergottite magmas were rich in Al and were saturated in plagioclase (e.g., QUE 94201, Los Angeles). This distinction in Al abundance appears to be a useful tool for classification.

High-Al Shergottites

Shergottites have been divided into two groups (Goodrich 2002): basalts (consisting of pyroxenes and plagioclase), and olivine-phyric basalts (with common large crystals of relatively magnesian olivine). However, the basaltic shergottites can be cleanly subdivided into high-Al and low-Al varieties, Fig. 1a (Table 1). The high-Al basalts contain 5–6.5% wt Al, which appears mineralogically as abundant plagioclase. The low-Al basalts contain 3.0–4.5% wt Al; mineralogically, they are dominated by pyroxenes. The olivine-phyric shergottites are not distinct in Al abundance from the low-Al basalt, but are distinct in containing magnesian olivine.

The distinction between high-Al and low-Al basalt shergottites extends to other major elements, and suggests that high-Al basalts are more fractionated than others. In a basaltic system fractionating olivine and low-Ca pyroxene (as do primitive shergottite magmas; Filiberto et al. 2012; Rapp et al. 2013), Al abundance and Fe/Mg ratio should increase together until an Al-saturated phase like plagioclase comes on the liquidus; this exact relation is seen in the shergottites, Fig. 1b. Al and Fe/Mg increase through the olivine-phyric and low-Al shergottites; the high-Al shergottites have essentially constant Al abundances over range of high Fe/Mg ratios. Similarly, Al+Ca increases through the olivine-phyric and low-Al basalts and is relatively constant for high-Al basalts. These correlations suggest that formation of the high-Al basalts involved plagioclase fractionation.

However, the distinction between high-Al and low-Al shergottites does not extend to incompatible trace elements (ITEs). As shown in Figs. 2 and 3, high-Al shergottites span the entire range of ITE enrichments known among all shergottites, from QUE 94201 at the low end, to Los Angeles at the high end.

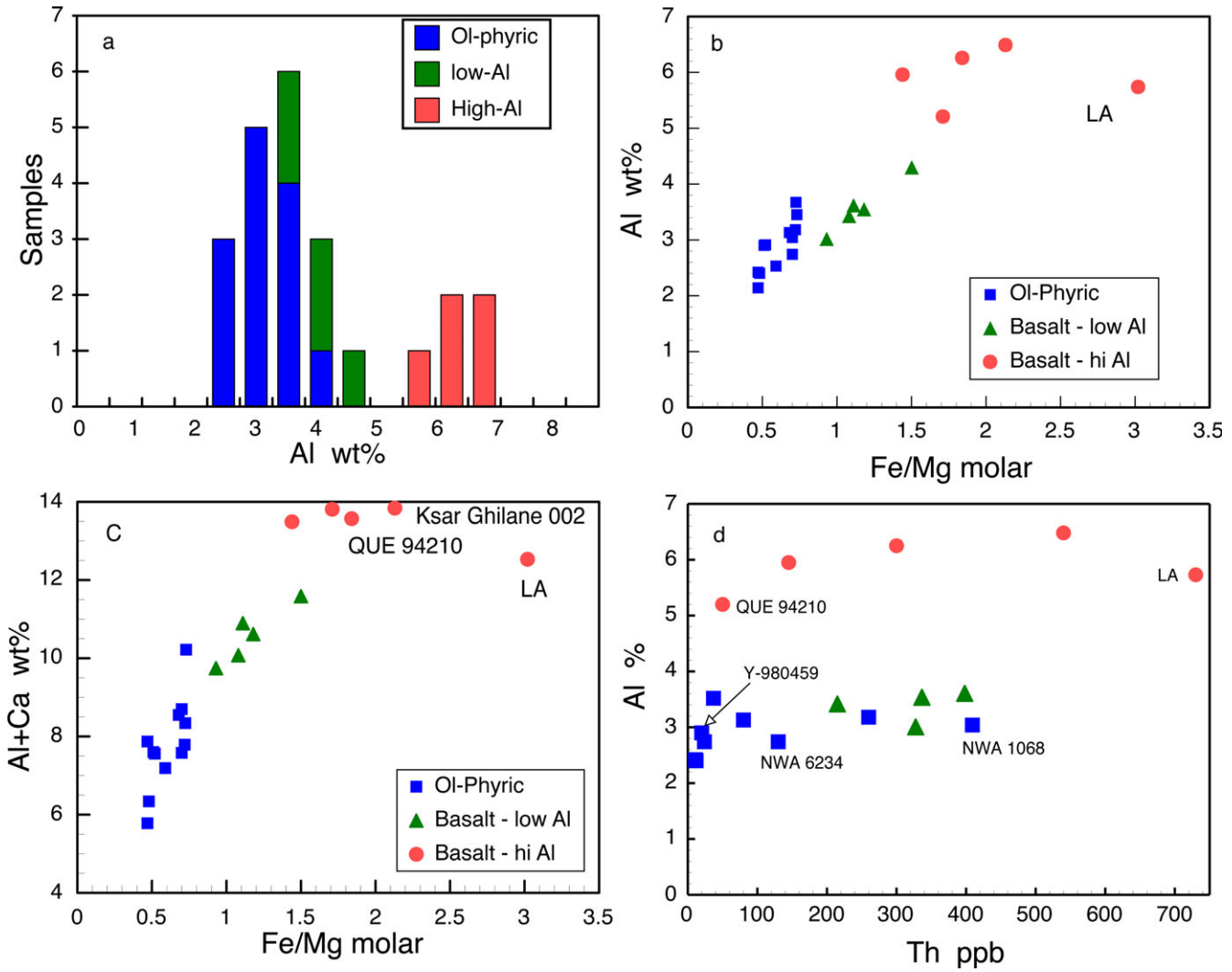

Fig. 1. Classification of shergottites by bulk chemistry and petrography. See Table 1 for samples plotted here and their classifications. a) Al contents of shergottite meteorites. The high-Al basalt group does not overlap at all with the low-Al and olivine-phyric basalts. b) Weight percent Al versus molar Fe/Mg for the shergottite varieties. Fe/Mg is a measure of degree of igneous fractionation—low values are more primitive. Al% wt increases with Fe/Mg through the olivine-phyric and low-Al basalts, as expected if Al behaved as an incompatible element. Al% wt is relatively constant for the high-Al shergottites, which suggests that they are all saturated in plagioclase. c) Weight percent Al+Ca versus molar Fe/Mg for the shergottite varieties. Al+Ca% wt is relatively constant for the high-Al shergottites, which suggests that they are saturated in plagioclase. d) Al versus Th, showing that shergottite basalt Al abundances are completely uncorrelated with those of highly incompatible elements (see Fig. 2).

Element Variation Patterns

A productive approach to understanding chemical and fractionation relationships among the shergottites is to seek regularities among their abundances of incompatible trace elements (e.g., Treiman et al. 1986; Treiman 2003). This represents a broader, though far less detailed, view than can be known from the radiogenic isotope systematics, like ^{147}Sm-^{143}Nd, and ^{176}Lu-^{176}Hf (e.g., Borg et al. 1997; Symes et al. 2008; Shafer et al. 2010). Geochemical events recorded by these (and other) radiogenic isotope systems must have had effects on the abundances of other elements, and possibly have left significant clues about the characteristics of those events.

The emphasis here is on refractory, lithophile, incompatible elements (as described in the Introduction); by considering these elements first, one focuses on silicate fractionation and mixing processes and avoids fractionations due to elemental volatility (e.g., related to planet formation, or basalt degassing) and siderophile behavior (e.g., related to metal

Table 1. Classifications of shergottite meteorites discussed here.

Olivine-Phyric	Low-Al	High-Al
DaG 489	NWA 480	Dho 378
Dho 019	NWA 856	EETA79001B
EETA79001A	Shergotty	Ksar Ghilane 002
LAR 06319	Zagami	Los Angeles (LA)
NWA 1068		QUE 94201
NWA 6234		
SaU 005		
Tissint		
Y-980459		
NWA 4925*	NWA 5298*	
NWA 5789*		
NWA 5990*		
NWA 6162*		

*Limited data available, e.g., no published trace element data.

separation as in core formation). In this work, we start with binary element variation diagrams, showing abundances of some target element versus those of a reference element, thorium (Fig. 2). Thorium is chosen because it is nearly perfectly incompatible in basaltic igneous processes, with partition coefficients $D^{Th}_{Min/basalt}$ near zero for nearly all minerals in basaltic systems (olivine, pyroxenes, plagioclase, Fe-Ti-oxides; Blundy and Wood 2003; Norman et al. 2005). Thus, Th abundances monitor the degree of silicate fractionation in basaltic systems. Thorium is compatible in phosphate minerals, apatite, and merrillite (Benjamin et al. 1983; Prowatke and Klemme 2006), and so is not suitable as a monitor of fractionation for low-volume melts (either partial or late stage).

The expected behavior of elements in such a binary diagram is shown in Fig. 2a. Consider a basalt with abundances of incompatible elements at point D. Removal of solid silicate minerals (as by fractionation) would concentrate both elements equally in the melt, and move its compositions away from the graph's origin (where the silicate minerals would plot). If the two elements in the diagram have significantly different compatibilities (e.g., if $D^{El}_{Min/basalt} = 0.5$), crystal fractionation would not yield a straight line from the origin, but a convex curve going up and right from the initial magma composition. Addition of silicate solids to a basaltic melt, as by accumulation, would move the system composition (magma + crystals) toward the origin—this is the case hypothesized for several olivine-phyric shergottites.

On this binary variation diagram, mixing of two components appears as a straight line between the two compositions, for example the heavy line between points D and E. The line between the two components need not extend to the origin; it will go to the origin only if the two chemical components have the same abundance ratios of the elements in question.

"Group 1" Elements

The "Group 1" elements of Treiman (2003), the most incompatible in silicate igneous petrogenesis, were seen to covary linearly among shergottite bulk compositions. This covariation is still apparent among the many more shergottites available now. Using Th as a reference element (Treiman [2003] used La), the shergottites define near-perfect correlations among abundances of Ta, U, La, Ce, and Nd (e.g., $R^2 = 0.970$ for Ta versus Th; $R^2 = 0.952$ for La versus Th; Figs. 2b–f). The other elements assigned to Group 1 by Treiman (2003) behave as do this subset; these other Group 1 elements include both refractory elements Ba, Be, Nb, and W, and the relatively volatile elements Li, K, Rb, Cs, Cl, and Br.

Refractory elements of Group 1 are not in the same relative abundances as in CI chondrites (Fig. 2). Among the element ratios in Fig. 2, Ta/Th and Ba/Th are at the CI value, but some element ratios are below that of CI, e.g., La/Th and K/Th. For refractory elements like La (Fig. 2d), the non-CI value of La/Th ratios cannot have arisen during crystal fractionation of olivine, pyroxene, etc., and arose during the early extreme depletions of incompatible elements in the shergottite source mantles (e.g., Borg et al. 2003). These depletions must predate the chemical variations among shergottites that are discussed here. For incompatible volatile elements like K (Fig. 2f), depletions relative to CI were established during the accretion of Mars (Dreibus and Wänke 1990; Treiman et al. 1986).

Several shergottites have abundances of some elements (e.g., U, Ce, or Ba; Figs. 2c and 2e) above their respective elements' main trends; these excesses can be attributed to terrestrial weathering (e.g., Korotev 2012).

"Group 2" Elements

Treiman et al. (1986) and Treiman (2003) noted that a second group of elements, of lesser incompatibility in silicate fractionations, had nearly constant abundance ratios. These "Group 2" elements included: Ti, heavy REE (e.g., Lu), Hf, Zr, Al, Ga, and Na (and others). The new data available here confirm most of the Group 2 correlations, see Fig. 3 (e.g., Lu, Hf, Ti, P), but reveal complications that were not apparent in the earlier data set. In effect, the earlier data set permitted several attractive hypotheses that are no longer supportable.

The first complication, compared to the analysis of Treiman (2003), is that the Group 2 element correlations do not pass through the origins of their respective graphs. This is clearest for P versus Ti (Fig. 3b), in which a linear correlation of the olivine-

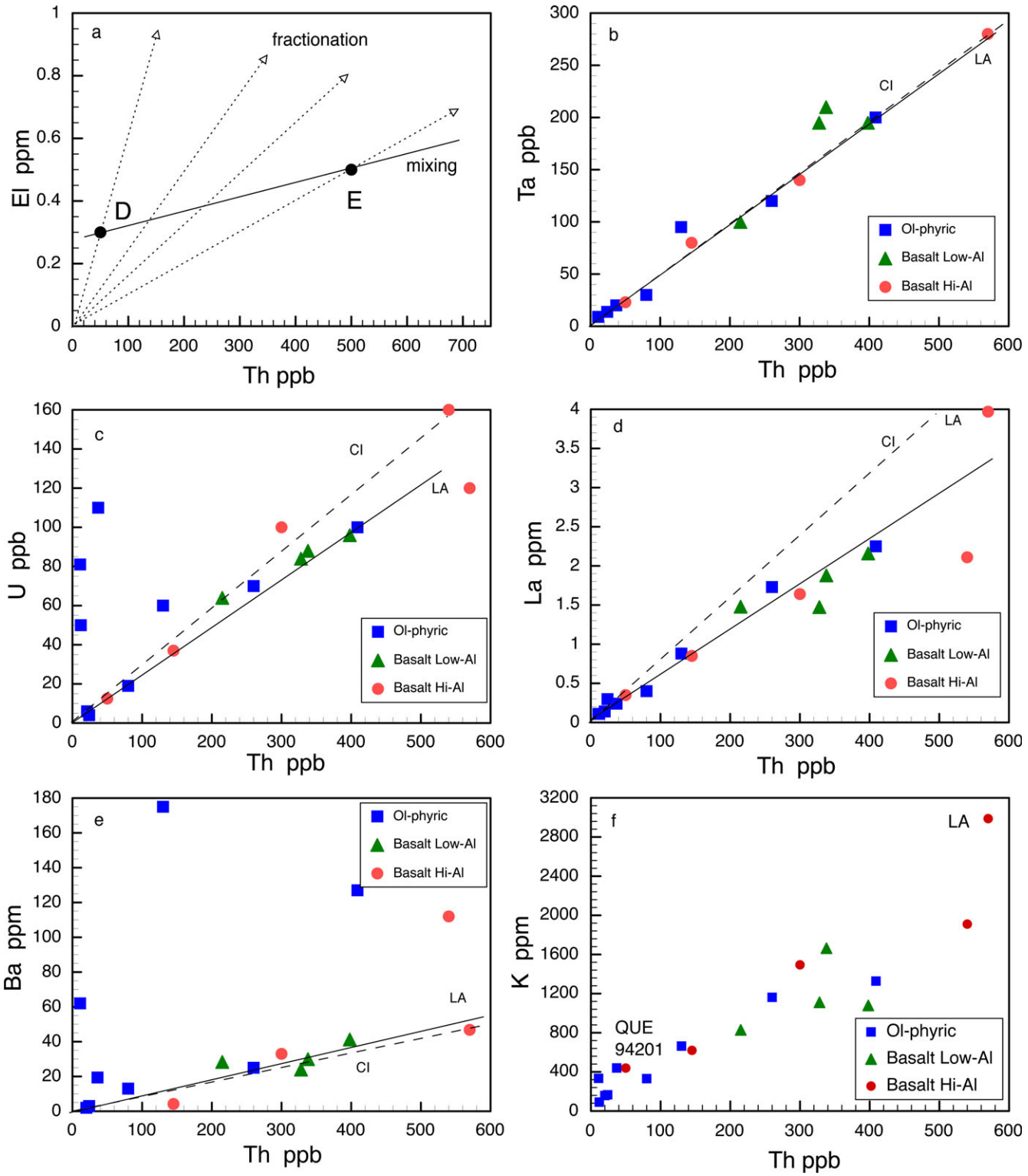

Fig. 2. Abundances of Group 1 elements versus Th. a) Schematic, showing the trajectory of mixing geochemical components (D & E) as the solid line, and trajectories of fractionation of olivine ± low-Ca pyroxene (arrows). b–f) Selected Group 1 elements. Solid lines are visual best fits through the data; dashed lines are at the CI ratio (Anders and Grevesse 1989). In parts c and e, high U and Ba values are ascribed to desert weathering and alteration.

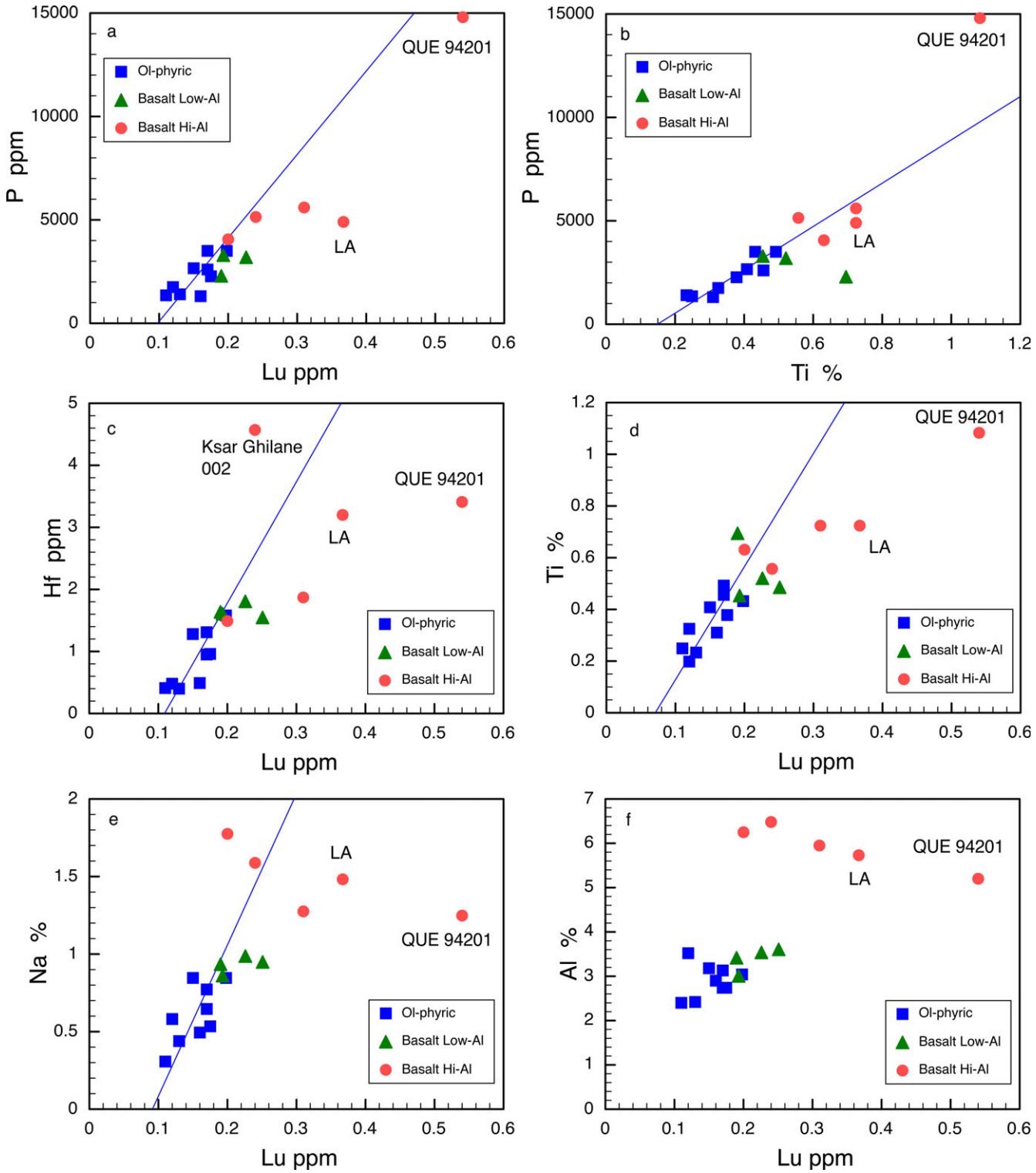

Fig. 3. Abundances of Group 2 elements versus Lu (except as noted). Blue lines are linear regressions through the olivine-phyric shergottite points (see text). a) P versus Lu. b) P versus Ti; compare with Fig. 3c of Treiman (2003). c) Hf versus Lu. Hf in Ksar Ghislaine 002 is anomalously elevated. d) Ti versus Lu. e) Na versus Lu; among high-Al basalts, Na is essentially independent of Lu. f) Al versus Lu; Al contents of high-Al basalts are disjunct from those of olivine-phyric and low-Al basalts, and do not correlate with Lu.

phyric data passes through P = 0% at Ti = 0.14% (R^2 = 0.83). Similar nonzero intercepts of linear correlations appear for: Hf versus Lu (Fig. 3c), Hf = 0 at Lu = 0.11 ppm (R^2 = 0.64); P versus Lu (Fig. 3b), P = 0 at Lu = 0.10 ppm (R^2 = 0.56); Ti versus Lu (Fig. 3d), Ti=0 at Lu=0.07 ppm (R^2 = 0.63); and Na versus Lu (Fig. 3e), Na=0 at Lu = 0.09 ppm (R^2 = 0.45). These nonzero intercepts are petrogenetically significant—Treiman (2003) forced an intercept at the origin to the graph of P versus Ti (his fig. 3c), found that the best explanation was that P behaved as less incompatible than Ti, and so explored phases and systems into which P might have been compatible (e.g., phosphide minerals in the Martian mantle). If one accepts a nonzero intercept as realistic, then this idea becomes unnecessary and the concept of multicomponent mixing becomes more palatable.

The second complication is that correlations among abundances of some Group 2 elements are apparent only for olivine-phyric and low-Al basalts, but do not necessarily extend to the high-Al basalts. The most striking of these noncorrelations are Na and Al, for which the high-Al basalts have relatively constant abundances over a wide range of Lu abundance (Figs. 3e and 3f). Presumably, the constancy of Al abundances is governed by plagioclase saturation in the high-Al basalts (see Classification section; Fig. 1c). Sodium abundances would also be buffered to some extent by plagioclase saturation, although Na is relatively incompatible in plagioclase (compared to Ca). Abundances of both Na and Al appear to decrease with increasing Lu (Figs. 3e and 3f), which seems counterintuitive for basalt saturated in (and buffered by) plagioclase. Perhaps, these trends represent a mass balance effect. As these basalts fractionate, they become enriched in the heavy elements Fe and Ti (along with Lu), so that the mass proportion of plagioclase decreases during fractionation, even if its volume proportion does not.

The third complication is that Al (and Ga) abundances are effectively uncorrelated with abundances of Lu or Ti (Fig. 3f), contrary to Treiman's (2003) finding of a strong correlation. Treiman's (2003) result was skewed by his inclusion of lherzolitic shergottites, which are cumulate rocks composed of accumulated olivine and low-Ca pyroxene with intercumulus parental magma. The lherzolites' Al, Lu, and Ti abundances would reflect mostly their proportion of intercumulus magma, and so would appear on diagrams like Fig. 3f as points between magma compositions and the origin.

"Group 2" versus "Group 1" Elements

In contrast, abundance ratios of elements in Group2/Group 1, see Fig. 4 (e.g., Sm/Th), are not relatively constant, as are ratios of those of Group1/Group1 (Fig. 2). Treiman (2003, figs. 2 and 5) saw that Group2/Group1 ratios fell into several distinct groups, each of which was interpreted as representing a distinct magma source (i.e., with distinct different values of Sm/La, P/La, etc.). This interpretation is no longer viable, because many of the shergottites discovered and analyzed since 2003 fall outside the sets of abundance ratios suggested by Treiman (2003), and imply rather that the shergottites span a continuum of values for these Group1/Group2 ratios. For example, abundance ratios of Sm/Th range nearly continuously from <1 × CI to approximately 9 × CI (Fig. 4a; compare with fig. 5b of Treiman 2003); however, abundance ratios Sm/La seem to have break between 4 × CI and 5 × CI, and appear to fall into three groups (Fig. 4b; depleted, >5 × CI; intermediate, 3–4 × CI; and enriched < 2 × CI; Filiberto et al. 2012). Filiberto et al. (2012) attributed this to three different source regions with possible mixing between these. However, it remains unclear if these breaks represent distinct groups of element ratios, or merely limited data; additional meteorites and analyses will be needed.

Mixing of several components seems to be a reasonable explanation for the ranges of Groups 1 versus 2 element ratios (Fig. 2a). For example, in Lu versus Th (Fig. 4c), most of the olivine-phyric shergottites fall along a line between the composition of Y-980459 (approximately 0.17 ppm Lu, approximately 20 ppb Th) and that of NWA 1068 (approximately 0.2 ppm Lu, approximately 410 ppb Th). This array is consistent with mixing of magma (or source) components, as in Fig. 2a, with one component like Y-980459 ("D" on Fig. 2a) the other like NWA 1068 ("E" on Fig. 2a), or with components on the same line, but more extreme than Y-980459 or NWA 1068. The low-Al basalts fall on or slightly above that mixing line (Fig. 4c), suggesting that their magmas (or sources) were generated in the same sort of mixing. Two groups of shergottites fall off the mixing line, and both can be explained simply and reasonably by crystal fractionation. First, several of the olivine-phyric shergottites fall below the mixing line, on their own line between the Y-980459 point and the origin. These compositions are consistent with addition of olivine to magmas like Y-980459 (i.e., the arrow on Fig. 4b between the QUE 94201 composition and the origin), as has been suggested for many of the olivine-phyric shergottites (see Filiberto et al. 2012).

The low-Al basalts fall on, or slightly above, the mixing line defined by the olivine-phyric basalts (Fig. 4), suggesting that they are fractionated only little from the olivine-phyric basalts. This is consistent with their Ca, Al, and Fe/Mg values (Fig. 1), which are slightly

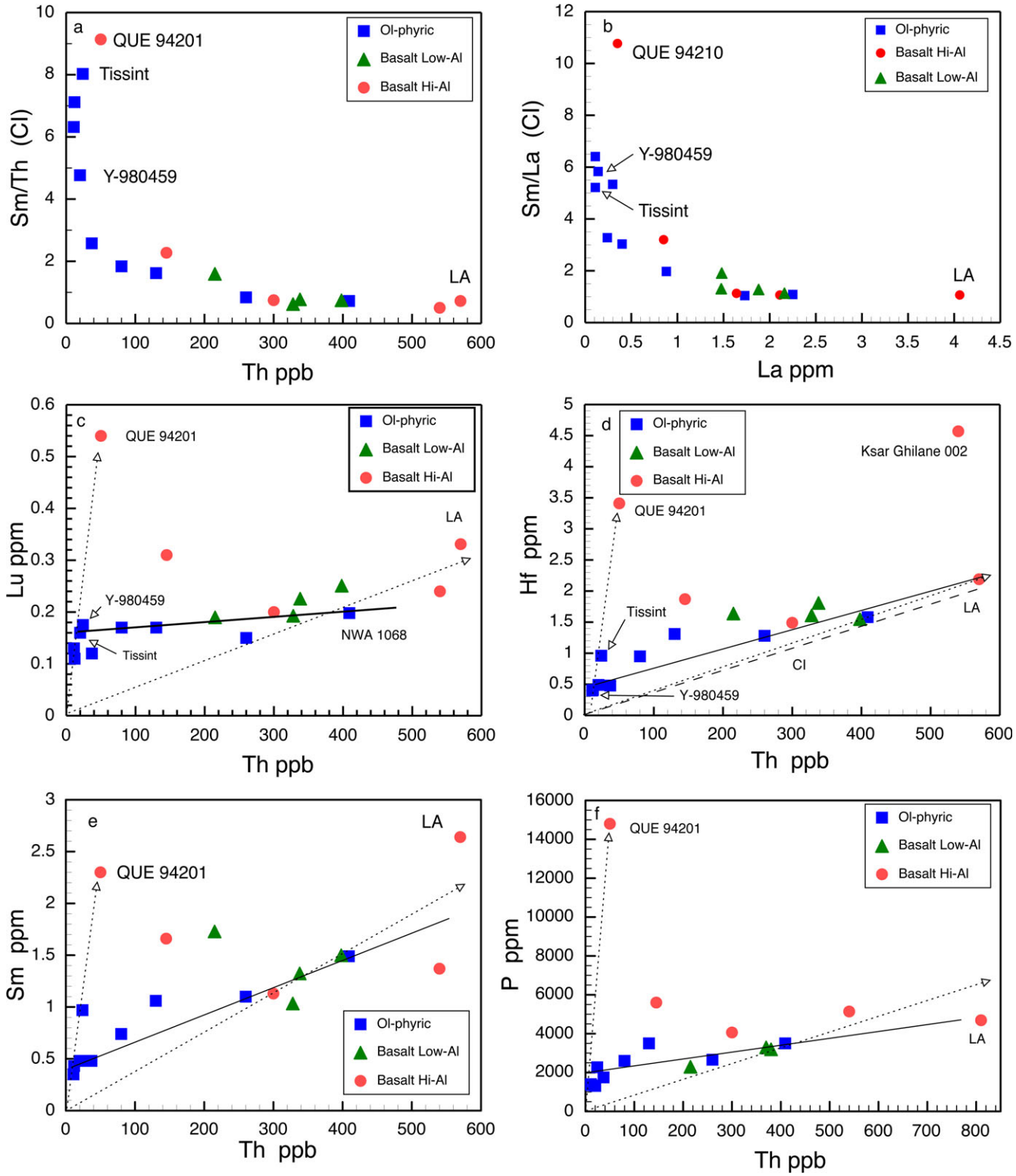

Fig. 4. Variation diagrams of Group 2 versus Group 1 elements, Th being taken as the reference element of Group 1 (Fig. 2). a) Sm/Th ratios normalized to CI; there is effectively a continuum of ratios, rather than the distinct sets of ratios as in Treiman (2003). b) Sm/La ratios, normalized to CI; the only gap in ratios is between QUE 94201 and the rest of the shergottites. c) Lu versus Th, the archetypal Group 2 and Group 1 elements. The olivine-phyric shergottites plot near a single line (solid), which could be ascribed to mixing. The high-Al shergottites QUE and Los Angeles plot in locations consistent with being fractionates of magmas like Y-980459 and NWA 1068, respectively. d) Hf versus Th. The Hf value for Ksar Ghilane 002 is aberrant (see Fig. 3c). e) Sm versus Th. f) P versus Th. For the Los Angeles meteorite, P and Th values are from Rubin et al. (2000).

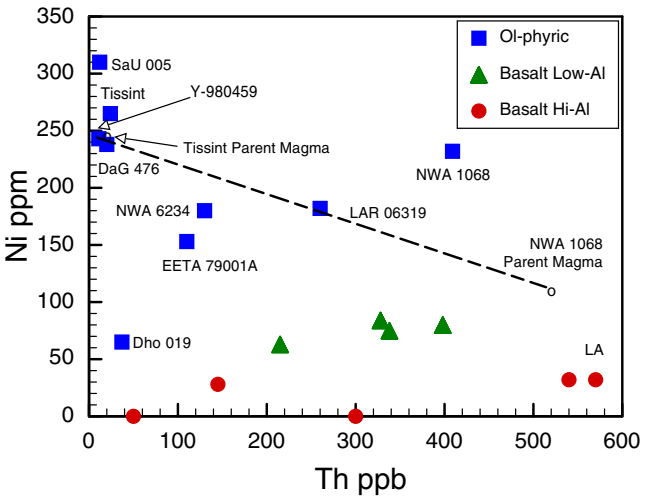

Fig. 5. Abundances of Ni and Th in shergottite basalts. The Tissint parent magma is calculated as the bulk composition −2% olivine megacrysts (Chennaoui Aoudjehane et al. 2013). The parent magma for NWA 1068 is calculated as the bulk composition −22% olivine megacrysts (Filiberto et al. 2010b).

greater than those of the olivine-phyric basalts. It is not clear, however, whether the degrees of fractionation implied by their trace element contents (Figs. 2–4) are consistent with those implied by their major element abundances (Fig. 1).

High-Al Basalt Origins

The high-Al shergottites plot above the mixing lines in Figs. 3 and 4, which can be understood as a result of fractionation of olivine (±low-Ca pyroxene) from magmas along the mixing line. The Los Angeles high-Al shergottite falls along lines from the graphs' origins through the NWA 1068 composition. To produce the former from the latter would have required enrichment of incompatible elements by approximately 70% (e.g., Fig. 2b), consistent with approximately 40% fractional crystallization (Raleigh fractionation; data of Table S1). This simple genetic relationship is permitted by their crystallization ages, which are both near approximately 180 Myr (Meyer 2012).

Similarly, the QUE 94201 shergottite falls along lines from the graphs' origins through the points for Y-980459 and Tissint. This colinearity suggests that QUE could have formed by fractionation of olivine, low-Ca pyroxene, and possibly plagioclase from a parental magma like Y-980459. To produce QUE 94201 from Y-980459 would have required enrichment of incompatible element abundances by approximately 3-fold, consistent with approximately 67% crystal fractionation (data of Table S1); however, the laboratory experiments of Rapp et al. (2013) imply much more extensive crystal fractionation (approximately 95%). QUE 94201 could not be a direct product of the Y-980459 magma because their crystallization ages are quite different, 327 Ma versus 472 Ma (Borg et al. 1997; Shih et al. 2005). However, QUE 94201 could conceivably have formed as a simple differentiate from the NWA 1195 magma, because their crystallization ages are within uncertainty of each other (Borg et al. 1997; Symes et al. 2008). Unfortunately, there are no complete chemical analyses of NWA 1195 (Meyer 2012), so it cannot be graphed on Figs. 2–4. Other possible parental olivine-phyric shergottites are significantly older than QUE 94201: Y-980459 at approximately 472 Ma (Shih et al. 2005), Tissint at approximately 596 Ma (Brennecka et al. 2014), SaU 005 at approximately 445 Ma (Shih et al. 2007), DaG 476 at approximately 474 Ma (Borg et al. 2003), Dho 019 at approximately 575 Ma (Borg et al. 2001), or NWA 5990 at approximately 400 Ma (Shih et al. 2011).

Compatible Element—Ni

Although our focus is on incompatible elements, abundances of the compatible element Ni provides significant constraints on the origins of the chemical components defined above, and provide a test of the two-component mixing hypothesis. Analyzed abundances of Ni are shown in Fig. 5a, compared to those of the archetypical Group 1 element Th. It should be noted that analyzed abundances of Ni may not be "true" bulk abundances because Ni is strongly concentrated in the large, dispersed crystals of magnesian olivine; a small aliquot for analysis could easily oversample or undersample these olivines, and thus over- or underestimate the true Ni content of the rock.

High-Al basalts contain nearly no Ni, consistent with their origins as products of significant crystal fractionation (olivine and low-Ca pyroxene). Low-Al basalts cluster around 70 ppm Ni despite their range of Th (200–400 ppb). The olivine-phyric basalts show the largest spread in Ni abundance, as might be expected from basalts inferred to have experienced accumulation and/or fractionation of olivine.

Ni in Mixing Components

To make sense of the diversity among olivine-phyric shergottites, we start with those inferred to represent melt compositions, or nearly so. Y-980459 is inferred to represent a magma composition based on liquidus experiments and mineral compositions (Ikeda 2004; Musselwhite et al. 2006; Shearer et al. 2008), and Tissint is inferred to represent a near-magma composition with only a few percent added olivine (Herd et al. 2013). Y-980459 and Tissint have similar Ni and Th abundances (Fig. 5a), and the inferred Tissint

melt composition (bulk Tissint −2% core olivine composition; Chennaoui Aoudjehane et al. 2013) is nearly identical to that of Y-980459. So, it makes sense to consider (as we have above) the composition of Y-980459 as representative of the depleted chemical component in the range of shergottites.

The NWA 5789 olivine-phyric shergottite is similar to Y-980459 in composition and texture (Gross et al. 2011), and has also been suggested to be a melt composition. Abundances of Ni (Irving et al. 2010) and Th (Mittlefehldt, personal communication) are also similar to those of Y-980459. Another similar olivine-phyric basalt is DaG 476 (and its pairs; Zipfel et al. 2000; Mikouchi et al. 2001; Wadhwa et al. 2001). However, it seems unlikely that DaG476 represents a melt composition, because the cores of its olivine crystals are too ferroan to have been in Fe/Mg equilibrium with a melt of the bulk composition (Mikouchi et al. 2001; Wadhwa et al. 2001; Filiberto and Dasgupta 2011). It must, then, be fortuitous that its Ni content is so similar to that of Y-980459.

The other chemical component, the enriched one, is taken above to have incompatible element abundances like NWA 1068, an olivine-phyric shergottite. NWA 1068 has nearly as much Ni as does Y-980459, but NWA 1068 is inferred to contain significant accumulated olivine, based on liquidus experiments and its mineral compositions (Filiberto et al. 2010a, 2010b). By Filiberto's experiments, essentially all of the olivine in NWA 1068 had accumulated into its parent magma. That inferred melt composition (bulk NWA 1068 −22% olivine; Filiberto et al. 2010a, 2010b; Shearer et al. 2008) gives an estimate of the parent melt composition as on Fig. 5a—with approximately 525 ppb Th and approximately 100 ppm Ni. This parent magma for NWA 1068 would seem more similar to low-Al basalts than other olivine-phyric basalts.

Ni in the Mixing Model

Having estimates of the Ni and Th abundances in the "depleted" and "enriched" components, we can test if other shergottite melt compositions could be mixtures of these components (recognizing uncertainty in the composition of the NWA 1068 parent melt). NWA 6234 is inferred to represent a melt composition, based on its bulk and olivine compositions (Gross et al. 2013), and it falls close to a mixing line between Y-980459 and the NWA 1068 parent melt (Fig. 5a). Another olivine-phyric shergottite, LAR 06319, falls essentially on the mixing line (in Ni and Th) of the two components (Fig. 5). LAR 06319 is inferred to be close to a magma composition, based on the compositions of its bulk, core olivines, and melt inclusions (Basu Sarbadhikari et al. 2009; Peslier et al. 2010), but may contain up to 10% excess olivine (Filiberto and Dasgupta 2011).

Exceptions

Two of the olivine-phyric basalts fall far from the mixing line between Y-980459 and the NWA 1068 parent composition, Fig. 5: Dho 019 and EETA79001A. Dho 019 is peculiar in containing only approximately 65 ppm Ni in bulk, but also containing approximately 10% of large magnesian olivine crystals (Fig. 5; Neal et al. 2001; Taylor et al. 2002). Olivine in Dho 019 also contains relatively little Ni compared to other olivine-phyric shergottites (Taylor et al. 2002). These facts suggest that Dho 019 arose from a source that contained significantly less Ni than the source(s) of Y-980459 and others, but had similar abundances (and abundance ratios) of incompatible elements. SaU 005 has approximately 25% more Ni than do Y-980459 and the Tissint parent magma, which is consistent with its high abundance of olivine megacrysts, 20–30% volume (Gnos et al. 2002; Goodrich 2003; Walton et al. 2005). The SaU olivine cores contain approximately 1100 ppm Ni (Shearer et al. 2008), so SaU 005 can be modeled (to zero-order) as a magma like Y-980459 plus approximately 8% olivine phenocrysts. EETA79001A is unique in containing xenoliths of harzburgite or lherzolite (olivine + low-Ca pyroxene ± plagioclase) and xenocrysts of olivine and low-Ca pyroxene (McSween and Jarosewich 1983; Shearer et al. 2013; but see Goodrich 2003); its position on Fig. 5 can thus be explained as being essentially a low-Al basalt with Ni-rich(er) xenocrysts.

IMPLICATIONS

Petrogenesis of Shergottites

Here, it has been shown that much of the diversity among the shergottite basalt meteorites can be explained in a simple petrogenetic scheme. First, olivine-phyric basalts were generated, with compositions consistent with mixtures of the Y-980459 meteorite composition (a melt composition), and the NWA 1068 meteorite composition (or its parent magma). The former is depleted in igneous incompatible elements, the latter is relatively enriched. The mixing could represent actual mixing of magmas or mixtures of source mantle materials, which were then melted. Fractionation of olivine from these magmas would raise their Al abundances and reduce their Mg/Fe, and yield (on exhaustion of olivine) low-Al basalts like Shergotty. Further fractionation (now of pyroxenes) would drive the residual melts to saturation in plagioclase, and yield high-Al basalt (like QUE 94201 and Los Angeles). This

scheme is consistent with the inference from radioisotope initials that the shergottite basalts represent mixtures (e.g., Borg and Draper 2003), and with inference from bulk compositions of significant silicate fractionations. However, this scheme is clearly an oversimplification of a complex set of magmatic events, stretching over >500 Myr (e.g., the Shergotty bulk composition has olivine on its liquidus, meaning it must be a cumulate and not a magma composition; Stolper and McSween 1979).

It is interesting that the range of incompatible element ratios across the olivine-phyric shergottites is the same as that in the high-Al shergottites. As exemplified in Fig. 4c, QUE 94201 and Y-980459 share the lowest Lu/Th ratio among the shergottite basalts, and Los Angeles and NWA 1068 share the highest Lu/Th ratio. The same pairing is seen in all other element ratios on Figs. 3 and 4. These facts suggest that the shergottites in hand sample the full range of geochemical variability (at least with respect to incompatible elements) in their source area(s) on Mars; otherwise we might have, for example, high-Al basalts with Lu/Th greater than that of Los Angeles and NWA 1068. If we now see the full range of geochemical variability in the shergottites that should permit significant constraints on magmatic processes that produced the variability.

This model for the shergottites, mixing of olivine-phyric magmas and/or their source regions followed by variable extents of crystal fractionation, can be extended (for the most part) to include the compatible element Ni. The most differentiated shergottites, the high-Al basalts, contain nearly no Ni; the low-Al basalts contain some, but significantly less than most of the olivine-phyric basalts (Fig. 5). These Ni abundances are consistent, in general, with the inference that the latter were parental to the former. Most of the olivine-phyric shergottites (or their parent magmas) have Ni and Th abundances consistent with mixing of a component like Y-980459 with a component like the NWA 1068 parent magma (Fig. 5); this relation is exactly as seen in the incompatible elements (Figs. 3 and 4). However, several of the olivine-phyric basalts contain too little Ni for consistency with this model, and suggest additional complexities. In particular, the low-Ni abundances of Dho 019 and its olivine crystals suggest the existence of primitive basalts with incompatible element abundances like those of Y-980459, but with approximately one quarter of the Ni (Fig. 5).

The enriched component in shergottite petrogenesis (i.e., like the NWA 1068 composition) has been likened to lunar KREEP based on its radiogenic isotopic compositions (e.g., Borg and Draper 2003; Borg et al. 2003, 2012; Jones 2003; Debaille et al. 2008). The lunar KREEP component is generally inferred to represent the last dregs of a magma ocean (but see Gross et al. 2014), and this Martian enriched component is taken as evidence that Mars experienced a magma ocean phase. The similarity of the Martian-enriched component and KREEP is confirmed by the data here on incompatible element abundances. Among the shergottites, abundances of refractory, lithophile, highly incompatible elements are not uniform relative to CI—i.e., they have been fractionated by igneous processes. Abundances of these elements show enrichments relative to CI in the order Th $\approx$ Ta > U > La > Ce > Nd (Fig. 2); this order and the elements' degrees of depletion are similar to those in lunar KREEP, Th $\approx$ U > La > Ce > Ta (Warren and Wasson 1979). The greater depletion of Ta in lunar KREEP may be ascribed to ilmenite fractionation in the lunar magma ocean, but not in comparable Martian petrogenesis.

Another important observation is that both the enriched and depleted components here (similar to those he recognized) have La/Th and La/U below the chondritic abundance ratios (McLennan 2003). If Mars's bulk composition has these refractory elements in the proportions of CIs, McLennan (2003) observed that Mars must contain another geochemical reservoir that has La/Th and La/U above the chondritic value. The abundance correlation diagrams here (Fig. 2) confirm this observation, and extend it to other incompatible elements. The identity of this missing component remains unclear.

Shergottites in Relation to Other Martian Basalts

While we do not have a full data set for rocks on the surface of Mars, spacecraft have returned chemical analyses of basalts, major elements, and some trace elements, from several locations (e.g., Gellert et al. 2006; Ming et al. 2008; Zipfel et al. 2011; Schmidt et al. 2014). These analyses have larger uncertainty because we do not have a full major, minor, and trace element suite; we cannot necessarily remove all alteration material; nor do we have detailed mineralogical analyses of these rocks. Yet, as a first-order comparison, we can compare K to Ti (an element of Group 1 versus one of Group 2) in the surface basalts with the shergottites. First, let us consider the shergottites alone (Fig. 6a); all classes of shergottites fall on a similar trend with basaltic shergottites containing more K and Ti and a nonzero intercept (similar to those in Fig. 4). This is consistent with crystal fractionation of olivine $\pm$ pyroxene from olivine-phyric shergottites to produce the more evolved basaltic shergottites.

Comparing the shergottites to the surface basalts (Fig. 6b), it is clear that most of the Mars surface

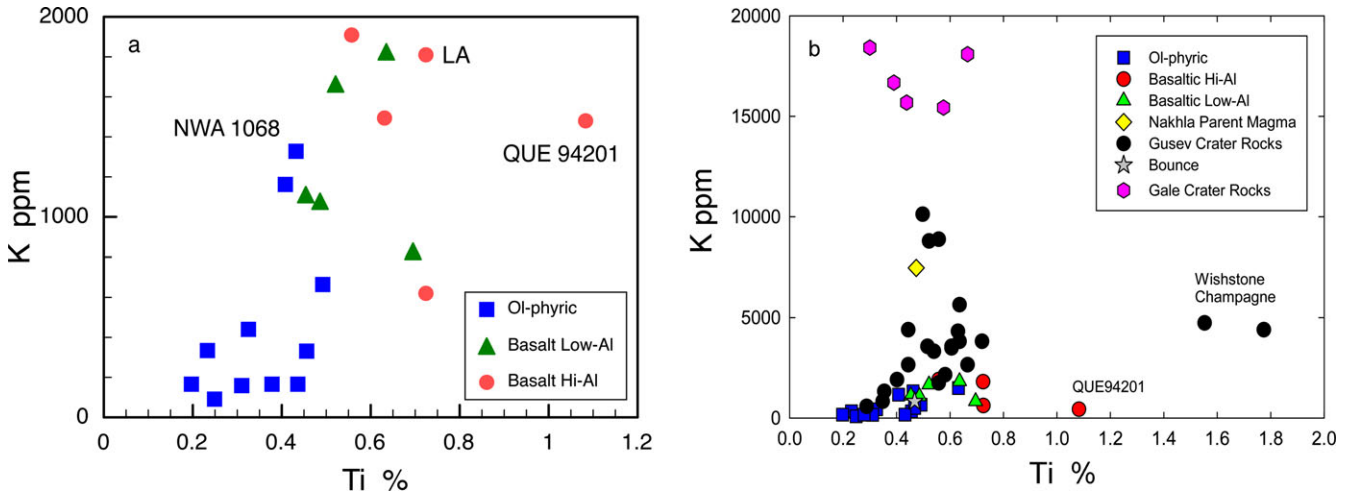

Fig. 6. Potassium and titanium abundances in shergottite basalts, part a, and compared with Mars surface basalts as analyzed by the MER and MSL rovers, part b (Ming et al. 2008; Zipfel et al. 2011; Schmidt et al. 2014).

basalts follow the same trends in K and Ti as the shergottites. The basalts analyzed in Gusev crater and the Bounce Rock in Meridiani Planum overlap the full range of shergottites and extend this range to higher K and Ti concentrations. However, two groups of Mars surface basalts are not represented among the known Martian meteorites. The Wishstone and Champagne rocks of Gusev crater (and their kin) are rich in Ti, and the Gale crater basaltic rocks are enriched in alkalis (Fig. 6b).

The Gusev crater basalts Wishstone and Champagne (and their kin) are anomalous in having a far higher Ti/K ratio than any of the other Martian basalts (Fig. 6b), and also are very rich in phosphorus (approximately 5 wt% P_2O_5; Usui et al. 2008). The high-Al basalt QUE 94201 is unusual among the Martian meteorites in being similarly, though not as extremely, enriched in Ti and P (approximately 3.5 wt% P_2O_5; Mikouchi et al. 1998). Wishstone-class basalts are thought to represent alkaline basalts similar to those of the Snake River Plain, Idaho (Usui et al. 2008), and a similar source region (or source region mixing) may be required to produce QUE 94201. Further data on trace elements from Wishstone-class type basalts would be needed to resolve this.

Basaltic rocks in Gale crater, Mars, analyzed by the APXS and ChemCam instruments on the Curiosity Rover, are alkali-rich relative to the Martian meteorites and most of the basalts of Gusev crater (Fig. 6b; Schmidt et al. 2014). A few rocks from the Home Plate outcrops at Gusev crater are similarly enriched in alkalis (Ming et al. 2008), and may be intermediate between "normal" Gusev basalts and the highly alkaline rocks of Gale (Fig. 6b). Significantly, the parental magma composition for the Nakhla Martian meteorite falls on this same trend (Fig. 6b), providing some linkage between the relatively alkali-poor shergottites and the highly alkaline rocks of Gale crater.

Acknowledgments—This line of work was begun in 1984 by AHT under the tutelage of Dr. Michael Drake, his post-doc advisor. AHT is grateful to Mike for his forbearance in starting on a project slightly outside the nominal source of funds, his trust that weeks of unsupervised work would eventually yield results, and his tolerance with a novice writer. We are grateful for the very helpful comments of C. Herd, S. Symes, and an anonymous reviewer, and the patience of the AE (N. Chabot) and guest AE (K. Righter). Supported in part by NASA grants NNX12AH64G to AT and NNX13AG35G to JF. LPI Contribution #1.

The authors declare that they have no conflicts of interest.

Editorial Handling—Dr. Nancy Chabot

REFERENCES

Agee C. B., Wilson N. V., McCubbin F. M., Ziegler K., Polyak V. J., Sharp Z. D., Asmerom Y., Nunn M. H., Shaheen R., Thiemens M. H., Steele A., Fogel M. L., Bowden R., Glamoclija M., Zhang Z., and Elardo S. M. 2013. Unique meteorite from early Amazonian Mars: Water-rich basaltic breccia Northwest Africa 7034. *Science* 339:780–785.

Anders E. and Grevesse N. 1989. Abundances of elements: Meteoritic and solar. *Geochimica et Cosmochimica Acta* 53:197–214.

Basu Sarbadhikari A., Day J. M. D., Liu Y., Rumble D. III, and Taylor L. A. 2009. Petrogenesis of olivine-phyric shergottite Larkman Nunatak 06319: Implications for enriched components in Martian basalts. *Geochimica et Cosmochimica Acta* 73:2190–2214.

Benjamin T. M., Jones J. H., Heuser W. R., and Burnett D. S. 1983. Laboratory actinide partitioning: Whitlockite/liquid and influence of actinide concentration levels. *Geochimica et Cosmochimica Acta* 43:1695–1705.

Blinova A. and Herd C. D. K. 2009. Experimental study of polybaric REE partitioning between olivine, pyroxene and melt of the Yamato 980459 composition: Insights into the petrogenesis of depleted shergottites. *Geochimica et Cosmochimica Acta* 73:3471–3492.

Blundy J. and Wood B. 2003. Mineral-melt partitioning of uranium, thorium and their daughters. *Reviews in Mineralogy and Geochemistry* 52:59–123.

Bogard D. D. and Johnson P. 1983. Martian gases in an Antarctic meteorite? *Science* 221:651–654.

Borg L. E. and Draper D. S. 2003. A petrogenetic model for the origin and compositional variation of the Martian basaltic meteorites. *Meteoritics & Planetary Science* 38:1713–1731.

Borg L. E., Nyquist L. E., Taylor L. A., Wisemann H., and Shih C.-Y. 1997. Constraints on martian differentiation processes from Rb-Sr and Sm-Nd isotopic analyses of the basaltic shergottite QUE 92410. *Geochimica et Cosmochimica Acta* 61:4915–4931.

Borg L. E., Nyquist L. E., Reese Y., Wiesmann H., Shih C. Y., Ivanova M., Nazarov M. A., and Taylor L. A. 2001. The age of Dhofar 019 and its relationship to the other Martian meteorites (abstract #1144). 32nd Lunar and Planetary Science Conference. CD-ROM.

Borg L. E., Nyquist L. E., Wiesmann H., Shih C.-Y., and Reese Y. 2003. The age of Dar al Gani 476 and the differentiation history of the Martian meteorites inferred from their radiogenic isotopic systematics. *Geochimica et Cosmochimica Acta* 67:3519–3536.

Borg L., Symes S., Marks N., Gaffney A., and Shearer C. 2012. Constraints on the composition and evolution of the Martian mantle from the isotopic systematics of basaltic meteorites. Workshop on the Mantle of Mars: Insights from Theory, Geophysics, High-Pressure Studies, and Meteorites, Abstract #6014. LPI Contribution 1684. Houston, Texas: Lunar and Planetary Institute.

Brennecka G. A., Borg L. E., Symes S. J. K., and Wadhwa M. 2014. Insights into the Martian mantle: The age and isotopics of the meteorite fall Tissint. *Meteoritics & Planetary Science* 49:412–418.

Bridges J. C. and Warren P. H. 2006. The SNC meteorites: Basaltic igneous processes on Mars. *Journal of the Geological Society* 163:229–251.

Burghele A., Dreibus G., Palme H., Rammensee W., Spettel B., Weckwerth G., and Wänke H. 1983. Chemistry of shergottites and the shergotty parent body (SPB): Further evidence for the two-component model of planet formation. Proceedings, 14th Lunar and Planetary Science Conference. pp. 80–81.

Chennaoui Aoudjehane H. C., Avice G., Barrat J. A., Boudouma O., Chen G., Duke M. J., Franchi I. A., Gattacecca J., Grady M. M., Greenwood R. C., Herd C. D. K., Hewins R., Jambon A., Marty B., Rochette P., Smith C. L., Sautter V., Verchovsky A., Weber P., and Zanda B. 2013. Tissint Martian meteorite: A fresh look at the interior, surface, and atmosphere of Mars. *Science* 33:785–788.

Debaille V., Yin Q. Z., Brandon A. D., and Jacobsen B. 2008. Martian mantle mineralogy investigated by the ^{176}Lu–^{176}Hf and ^{147}Sm–^{143}Nd systematics of shergottites. *Earth and Planetary Science Letters* 269:186–199.

Drake M. J. 2000. Accretion and primary differentiation of the Earth: A personal journey. *Geochimica et Cosmochimica Acta* 64:2367–2370.

Drake M. J. and Righter K. 2002. Determining the composition of the Earth. *Nature* 416:39–44.

Dreibus G. and Wänke H. 1985. Mars, a volatile-rich planet. *Meteoritics* 20:367–381.

Dreibus G. and Wänke H. 1987. Volatiles on Earth and Mars: A comparison. *Icarus* 71:225–240.

Dreibus G. and Wänke H. 1990. Comparison of the chemistry of Moon and Mars. *Advances in Space Research* 10:7–16.

Filiberto J. and Dasgupta R. 2011. Fe^{2+}-Mg partitioning between olivine and basaltic melts: Applications to genesis of olivine-phyric shergottites and conditions of melting in the Martian interior. *Earth and Planetary Science Letters* 304:527–537.

Filiberto J., Dasgupta R., Kiefer W. S., and Treiman A. H. 2010a. High pressure, near-liquidus phase equilibria of the Home Plate basalt Fastball and melting in the Martian mantle. *Geophysical Research Letters* 37:L13201.

Filiberto J., Musselwhite D., Gross J., Burgess K., Le L., and Treiman A. H. 2010b. Experimental petrology, crystallization history, and parental magma characteristics of olivine-phyric shergottite NWA 1068: Implications for the petrogenesis of "enriched" olivine-phyric shergottites. *Meteoritics & Planetary Science* 45:1258–1270.

Filiberto J., Chin E., Day J. M. D., Gross J., Penniston-Dorland S., Schwenzer S. P., Greenwood R., and Treiman A. H. 2012. Geochemistry of intermediate olivine-phyric shergottite Northwest Africa 6234 with similarities to basaltic shergottite Northwest Africa 480 and olivine-phyric shergottite Northwest Africa 2990. *Meteoritics & Planetary Science* 47:1–17.

Foley C. N., Wadhwa M., Borg L. E., Janney P. E., Hines R., and Grove T. L. 2005. The early differentiation history of Mars from ^{182}W-^{142}Nd isotope systematics in the SNC meteorites. *Geochimica et Cosmochimica Acta* 69:4557–4571.

Gellert R., Rieder R., Bruckner J., Clark B. C., Dreibus G., Klingelhöfer G., Lugmair G., Ming D. W., Wänke H., Yen A., Zipfel J., and Squyres S. W. 2006. Alpha particle X-ray spectrometer (APXS): Results from Gusev crater and calibration report. *Journal of Geophysical Research* 111:E2. doi:10.1029/2005JE002555.

Gnos E., Hofmann B., Franchi I. A., Al-Kathiri A., Huser M., and Moser L. 2002. Sayh al Uhaymir 094: A new martian meteorite from the Oman desert. *Meteoritics & Planetary Science* 37:835–854.

Goodrich C. A. 2002. Olivine–phyric Martian basalts: A new type of shergottite. *Meteoritics & Planetary Science* 37: B31–B34.

Goodrich C. A. 2003. Petrogenesis of olivine-phyric shergottites Sayh al Uhaymir 005 and Elephant Moraine A79001 lithology A. *Geochimica et Cosmochimica Acta* 67:3735–3772.

Greenough J. D. and Ya'akoby A. 2013. A comparative geochemical study of Mars and Earth basalt petrogenesis. *Canadian Journal of Earth Science* 50:3045–3057.

Gross J., Treiman A. H., Filiberto J., and Herd C. D. K. 2011. Primitive olivine-phyric shergottite NWA 5789: Petrography, mineral chemistry, and cooling history imply

a magma similar to Yamato-980459. *Meteoritics & Planetary Science* 46:116–133.

Gross J., Filiberto J., Herd C. D. K., Melwani Daswani M., Schwenzer S. P., and Treiman A. H. 2013. Petrography, mineral chemistry, and crystallization history of olivine-phyric shergottite NWA 6234: A new intermediate melt composition. *Meteoritics & Planetary Science* 48:854–871.

Gross J., Treiman A. H., and Mercer C. N. 2014. Lunar feldspathic meteorites: Constraints on the geology of the lunar highlands, and the origin of the lunar crust. *Earth and Planetary Science Letters* 388:318–328.

Herd C. D. 2003. The oxygen fugacity of olivine-phyric Martian basalts and the components within the mantle and crust of Mars. *Meteoritics & Planetary Science* 38:1793–1805.

Herd C. D. K., Borg L. E., Jones J. H., and Papike J. J. 2002. Oxygen fugacity and geochemical variations in the Martian basalts: Implications for Martian basalt petrogenesis and the oxidation state of the upper mantle of Mars. *Geochimica et Cosmochimica Acta* 66:2025–2036.

Herd C. D. K., Duke M. J. M., Bryden C. D., and Pearson D. G. 2013. Tissint among the shergottites: Parental melt composition, redox state, La/Yb and V/Sc (abstract #2840). 44th Lunar and Planetary Science Conference. CD-ROM.

Hillgren V. J., Drake M. J., and Rubie D. C. 1996. High pressure and high temperature metal-silicate partitioning of siderophile elements: The importance of silicate liquid composition. *Geochimica et Cosmochimica Acta* 60:2257–2263.

Ikeda Y. 2004. Petrology of the Y980459 shergottite. *Antarctic Meteorite Research (Japan)* 17:35–54.

Irving A. J., Kuehner S. M., Herd C. D. K., Gellissen M., Korotev R. L., Puchtel I., Walker R. J., Lapen T., and Rumble D. 2010. Petrologic, elemental and multi-isotopic characterization of permafic olivine-phyric shergottite Northwest Africa 5789: A primitive magma derived from depleted Martian mantle (abstract #1547). 41st Lunar and Planetary Science Conference. CD-ROM.

Irving A., Herd C. D. K., Gellissen M., Kuehner S., and Bunch T. 2011. Paired fine grained, permafic olivine-phyric shergottites northwest Africa 2990/5960/6234/6710: Trace element evidence for a new type of Martian mantle source or complex lithospheric assimilation processes (abstract #5232). *Meteoritics & Planetary Science* 46:A108.

Jambon A., Barrat J. A., Sautter V., Gillet P., Gpel C., Javoy M., Joron J. L., and Lesourd M. 2002. The basaltic shergottite Northwest Africa 856: Petrology and chemistry. *Meteoritics & Planetary Science* 37:1147–1164.

Jones J. H. 1984. The composition of the mantle of the eucrite parent body and the origin of eucrites. *Geochimica et Cosmochimica Acta* 48:641–648.

Jones J. H. 1989. Isotopic relationships among the shergottites, the nakhlites and Chassigny. 19th Lunar and Planetary Science Conference. pp. 465–474.

Jones J. H. 2003. Constraints on the structure of the martian interior determined from the chemical and isotopic systematics of SNC meteorites. *Meteoritics & Planetary Science* 38:1807–1814.

Jones J. H. and Drake M. J. 1993. Rubidium and cesium in the Earth and the Moon. *Geochimica et Cosmochimica Acta* 57:3785–3792.

Korotev R. L. 2012. Lunar meteorites from Oman. *Meteoritics & Planetary Science* 47:1365–1402.

McCubbin F. M., Elardo S. M., Shearer C. K., Smirnov A., Hauri E. H., and Draper D. S. 2013. A petrogenetic model for the comagmatic origin of chassignites and nakhlites: Inferences from chlorine-rich minerals, petrology, and geochemistry. *Meteoritics & Planetary Science* 48:819–853.

McLennan S. M. 2003. Large-ion lithophile element fractionation during the early differentiation of Mars and the composition of the Martian primitive mantle. *Meteoritics & Planetary Science* 38:895–904.

McSween H. Y. Jr. and Jarosewich E. 1983. Petrogenesis of the EETA79001 meteorite: Multiple magma pulses on the shergottite parent body. *Geochimica et Cosmochimica Acta* 47:1501–1513.

Meyer C. 2012. Mars Meteorite Compendium, Updated. http://curator.jsc.nasa.gov/antmet/mmc/index.cfm. Accessed January 2014.

Mikouchi T., Miyamoto M., and McKay G. A. 1998. Mineralogy of Antarctic basaltic shergottite QUE 94201: Similarities to EETA7900 1 (Lithology B) Martian meteorite. *Meteoritics & Planetary Science* 33:181–189.

Mikouchi T., Miyamoto M., and McKay G. A. 2001. Mineralogy and petrology of the Dar al Gani 476 Martian meteorite: Implications for its cooling history and relationship to other shergottites. *Meteoritics & Planetary Science* 36:531–548.

Ming D. W., Gellert R., Morris R. V., Arvidson R. E., Brückner J., Clark B. C., Cohen B. A., d'Uston C., Economou T., Fleischer I., Klingelhöfer G., McCoy T. J., Mittlefehldt D. W., Schmidt M. E., Schröder C., Squyres S. W., Tréguier E., Yen A. S., and Zipfel J. 2008. Geochemical properties of rocks and soils in Gusev Crater, Mars: Results of the Alpha Particle X-Ray Spectrometer from Cumberland Ridge to Home Plate. *Journal of Geophysical Research* 113:E12S39.

Musselwhite D. S., Dalton H. A., Kiefer W. S., and Treiman A. H. 2006. Experimental petrology of the basaltic shergottite Yamato-980459: Implications for the thermal structure of the Martian mantle. *Meteoritics & Planetary Science* 41:1271–1290.

Neal C. R., Taylor L. A., Ely J. C., Jain J. C., and Nazarov M. A. 2001. Detailed geochemistry of new shergottite Dhofar 019 (abstract #1671). 32nd Lunar and Planetary Science Conference. CD-ROM.

Newsom H. E. and Drake M. J. 1982. The metal content of the eucrite parent body: Constraints from the partitioning behavior of tungsten. *Geochimica et Cosmochimica Acta* 46:2483–2489.

Newsom H. E. and Palme H. 1984. The depletion of siderophile elements in the Earth's mantle: New evidence from molybdenum and tungsten. *Earth and Planetary Science Letters* 69:354–364.

Norman M., Garcia M. O., and Pietruszka A. J. 2005. Trace-element distribution coefficients for pyroxenes, plagioclase, and olivine in evolved tholeiites from the 1955 eruption of Kilauea Volcano, Hawai'i, and petrogenesis of differentiated rift-zone lavas. *American Mineralogist* 90:888–899.

Peslier A. H., Hnatyshin D., Herd C. D. K., Walton E. L., Brandon A. D., Lapen T. J., and Shafer J. T. 2010. Crystallization, melt inclusion, and redox history of a Martian meteorite: Olivine-phyric shergottite Larkman Nunatak 06319. *Geochimica et Cosmochimica Acta* 74:4543–4576.

Prowatke S. and Klemme S. 2006. Trace element partitioning between apatite and silicate melts. *Geochimica et Cosmochimica Acta* 70:4513–4527.

Rapp J. F., Draper D. S., and Mercer C. M. 2013. Anhydrous liquid line of descent of Yamato-980459 and evolution of Martian parental magmas. *Meteoritics & Planetary Science* 48:1780–1799.

Righter K. and Drake M. J. 1997. A magma ocean on Vesta: Core formation and petrogenesis of eucrites and diogenites. *Meteoritics & Planetary Science* 32:929–944.

Righter K. and Drake M. J. 2003. Partition coefficients at high pressure and temperature. In *The mantle and core*, edited by Carlson C. W., Holland H., and Turekian K. Treatise on Geochemistry, Vol. 2. Amsterdam: Elsevier. pp. 425–449.

Rubin A. E., Warren P. H., Greenwood J. P., Verish R. S., Leshin L. A., Hervig R. L., Clayton R. N., and Mayeda T. K. 2000. Los Angeles: The most differentiated basaltic Martian meteorite. *Geology* 28:1011–1014.

Schmidt M. E., Campbell J. L., Gellert R., Perrett G. M., Treiman A. H., Blaney D. L., Olilla A., Calef F. J., Edgar L., Elliott B. E., Grotzinger J., Hurowitz J., King P. L., Minitti M. E., Sautter V., Stack K., Berger J. A., Bridges J. C., Ehlmann B. L., Forni O., Leshin L. A., Lewis K. W., McLennan S. M., Ming D. W., Newsom H., Pradler I., Squyres S. W., Stolper E. M., Thompson L., Van Bommel S., and Wiens R. C. 2014. Geochemical diversity in first rocks examined by the Curiosity Rover in Gale Crater: Evidence for and significance of an alkali and volatile-rich igneous source. *Journal of Geophysical Research: Planets* 119:2013JE004481.

Shafer J. T., Brandon A. D., Lapen T. J., Righter M., Peslier A. H., and Beard B. L. 2010. Trace element systematics and ^{147}Sm–^{143}Nd and ^{176}Lu–^{176}Hf ages of Larkman Nunatak 06319: Closed-system fractional crystallization of an enriched shergottite magma. *Geochimica et Cosmochimica Acta* 74:7307–7328.

Shearer C. K., Burger P. V., Papike J. J., Borg L. E., Irving A. J., and Herd C. D. K. 2008. Petrogenetic linkages among Martian basalts: Implications based on trace element chemistry of olivine. *Meteoritics & Planetary Science* 43:1241–1258.

Shearer C. K., Aaron P. M., Burger P. V., Guan Y., Bell A. S., and Papike J. J. 2013. Petrogenetic linkages among fO_2, isotopic enrichments-depletions and crystallization history in Martian basalts. Evidence from the distribution of phosphorus in olivine megacrysts. *Geochimica et Cosmochimica Acta* 120:17–38.

Shih C. Y., Nyquist L. E., Bogard D. D., McKay G. A., Wooden J. L., Bansal B. M., and Wiesmann H. 1982. Chronology and petrogenesis of young achondrites, Shergotty, Zagami, and ALHA77005: Late magmatism on a geologically active planet. *Geochimica et Cosmochimica Acta* 46:2323–2344.

Shih C.-Y., Nyquist L. E., Wiesmann H., Reese Y., and Misawa K. 2005. Rb-Sr and Sm-Nd dating of olivine-phyric shergottite Yamato 980459: Petrogenesis of depleted shergottites. *Antarctic Meteorite Research (Japan)* 18:46–65.

Shih C.-Y., Nyquist L. E., and Reese Y. 2007. Rb-Sr and Sm-Nd isotopic studies of Martian depleted shergottites SaU 094/005 (abstract #1745). 38th Lunar and Planetary Science Conference. CD-ROM.

Shih C-Y., Nyquist L. A., Reese Y., and Irving A. 2011. Rb-Sr and Sm-Nd ages, and petrogenesis of depleted shergottite Northwest Africa 5990 (abstract #1846). 42nd Lunar and Planetary Science Conference. CD-ROM.

Stolper E. M. and McSween H. Y. Jr 1979. Petrology and origin of the shergottite meteorites. *Geochimica et Cosmochimica Acta* 43:1475–1498.

Symes S. J., Borg L. E., Shearer C. K., and Irving A. J. 2008. The age of the Martian meteorite Northwest Africa 1195 and the differentiation history of the shergottites. *Geochimica et Cosmochimica Acta* 72:1696–1710.

Taylor L. A., Nazarov M. A., Shearer C. K., McSween H. Y., Cahill J., Neal C. R., Ivanova M. A., Barsukova L.D., Lentz R. C., Clayton R. N., and Mayeda T. K. 2002. Martian meteorite Dhofar 019: A new shergottite. *Meteoritics & Planetary Science* 37:1107–1128.

Treiman A. H. 2003. Chemical compositions of Martian basalts (shergottites): Some inferences on basalt formation, mantle metasomatism, and differentiation in Mars. *Meteoritics & Planetary Science* 38:1849–1864.

Treiman A. H., Drake M. J., Janssens M.-J., Wolf R., and Ebihara M. 1986. Core formation in the Earth and Shergottite Parent Body (SPB): Chemical evidence from basalts. *Geochimica et Cosmochimica Acta* 50:1071–1091.

Treiman A. H., Jones J. H., and Drake M. J. 1987. Core formation in the Shergottite Parent Body: A chemical model. Proceedings, 17th Lunar and Planetary Science Conference. *Journal of Geophysics Research Supplement* 92: E627–E632.

Treiman A. H., Gleason J. D., and Bogard D. D. 2000. The SNC meteorites are from Mars. *Planetary and Space Science* 48:1213–1230.

Usui T., McSween H. Y. Jr., and Clark III B. C. 2008. Petrogenesis of high-phosphorous Wishstone Class rocks in Gusev Crater, Mars. *Journal of Geophysical Research: Planets* 113:E12S44. doi:10.1029/2008JE003225.

Wadhwa M., Lentz R. C. F., McSween H. Y. Jr., and Crozaz G. 2001. A petrologic and trace element study of Dar al Gani 476 and Dar al Gani 489: Twin meteorites with affinities to basaltic and Iherzolitic shergottites. *Meteoritics & Planetary Science* 36:195–208.

Walton E. L., Spray J. G., and Bartoschewitz R. 2005. A new Martian meteorite from Oman: Mineralogy, petrology, and shock metamorphism of olivine-phyric basaltic shergottite Sayh al Uhaymir 150. *Meteoritics & Planetary Science* 40:1195–1214.

Wänke H. 1981. Constitution of the terrestrial planets. *Philosophical Transactions of the Royal Society of London A* 303:287–302.

Wänke H. and Dreibus G. 1988. Chemical composition and accretion history of terrestrial planets. *Philosophical Transactions Royal Society London A* 325:545–557.

Wänke H., Baddenhausen H., Balacescu A., Teschke F., Spettel B., Dreibus G., Palme H., Quijano-Rico M., Kruse H., Wlotzka F., and Begemann F. 1972. Multielement analyses of lunar samples and some implications of the results. Proceedings, 3rd Lunar Science Conference. pp. 1251–1268.

Wänke H., Baddenhausen H., Dreibus G., Quijano-Rico M., Palme H., Spettel B., and Teschke F. 1973. Multielement analysis of Apollo 16 samples and about the composition of the whole moon. Proceedings, 4th Lunar Science Conference. pp. 761–763.

Warren P. H. and Wasson J. T. 1979. The origin of KREEP. *Reviews of Geophysics and Space Physics* 17:73–88.

Zipfel J., Scherer P., Spettel B., Dreibus G., and Schultz L. 2000. Petrology and chemistry of the new shergottite Dar al Gani 476. *Meteoritics & Planetary Science* 35: 95–106.

Zipfel J., Schröder C., Jolliff B. L., Gellert R., Herkenhoff K. E., Rieder R., Anderson R., Bell J. F., Brückner J., Crisp J. A., Christensen P. R., Clark B. C., De Souza P. A. Jr., Dreibus G., D'Uston C., Economou T., Gorevan S. P., Hahn B. C., Klingelhöfer G., McCoy T. J., McSween H. Y. Jr., Ming D. W., Morris R. V., Rodionov D. S., Squyres S. W., Wänke H., Wright S. P., Wyatt M. B., and Yen A. S. 2011. Bounce Rock—A shergottite-like basalt encountered at Meridiani Planum, Mars. *Meteoritics & Planetary Science* 46:1–20.

SUPPORTING INFORMATION

Additional supporting information may be found in the online version of this article:

Table S1: Major- and trace-element abundance data for olivine-phyric and basaltic shergottites. Modified after supplement in Filiberto et al. (2012).